Computer Aided Diagnosis of Clustered Microcalcifications Using Artificial Neural Nets*

Erich Sorantin[1], Ferdinand Schmidt[1], Heinz Mayer[1], Michael Becker[1], Csaba Szepesvári[2], Ewald Graif[1], Peter Winkler[1]

[1] Department of Radiology, Univ.Hospital Graz, Auenbruggerplatz 34, A- 8036 Graz, Austria
[2] Research Group on Artificial Intelligence, "Joszef Attila" University Szeged, Aradi vrt. tere 1, H-6720 Hungary

Objective: Development of a fully automated computer application for detection and classification of clustered microcalcifications using neural nets.

Material and Methods: Mammographic films with clustered microcalcifications of known histology were digitized. All clusters were rated by two radiologists on a 3 point scale: benign, indeterminate and malignant. Automated detected clustered microcalcifications were clustered. Features derived from those clusters were used as input to 2 artificial neural nets: one was trained to identify the indeterminate clusters, whereas the second ANN classified the remaining clusters in benign or malignant ones. Performance evaluation followed the patient-based receiver operator characteristic analysis.

Results: For identification of patients with indeterminate clusters a an Az-value of 0.8741 could be achieved. For the remaining patients their clusters could be classified as benign or malignant at an Az-value of 0.8749, a sensitivity of 0.977 and specificity of 0.471.

Conclusions: A fully automated computer system for detection and classification of clustered microcalcifications was developed. The system is able to identify patients with indeterminate clusters, where additional investigations are recommended, and produces a reliable estimation of the biologic dignity for the remaining ones.

Introduction

Breast carcinoma is the main cause of deaths in women suffering from cancer. Its early detection is vital in order to improve its prognosis [1]. Screen film mammography is the method of choice today and the only accepted screening modality. Clustered microcalcifications (MCS) are one of the mammographic hallmarks of early breast cancer [2]. However not all MCS are in indication of malignancy, since they can occur during the course of other benign diseases too. In addition similar looking artefacts must be differentiated from MCS [3,4,5]. Digital mammography is just at the beginning of its commercialization. These systems will allow immediate digital image processing to assist the reporting radiologist for both, detection and classification of MCS [6]. Several algorithms for detecting MCS have already been published [2,7,8,9]. Only a few reports deal with computer aided classification of clustered MCS [10,11,12]. Those reports use either manual identification of MCS for computer assisted feature extraction [11] or human feature extraction [10,12] as an input for their classification systems. Both approaches are time consuming and bear the burden of human subjectivity.

The goal of this study was to develop a fully automated computer application for detection and classification of clustered MCS, using artificial neural nets (ANNs).

Materials and Methods

The database consisted of 272 mammographic films of 100 patients with suspicious clustered
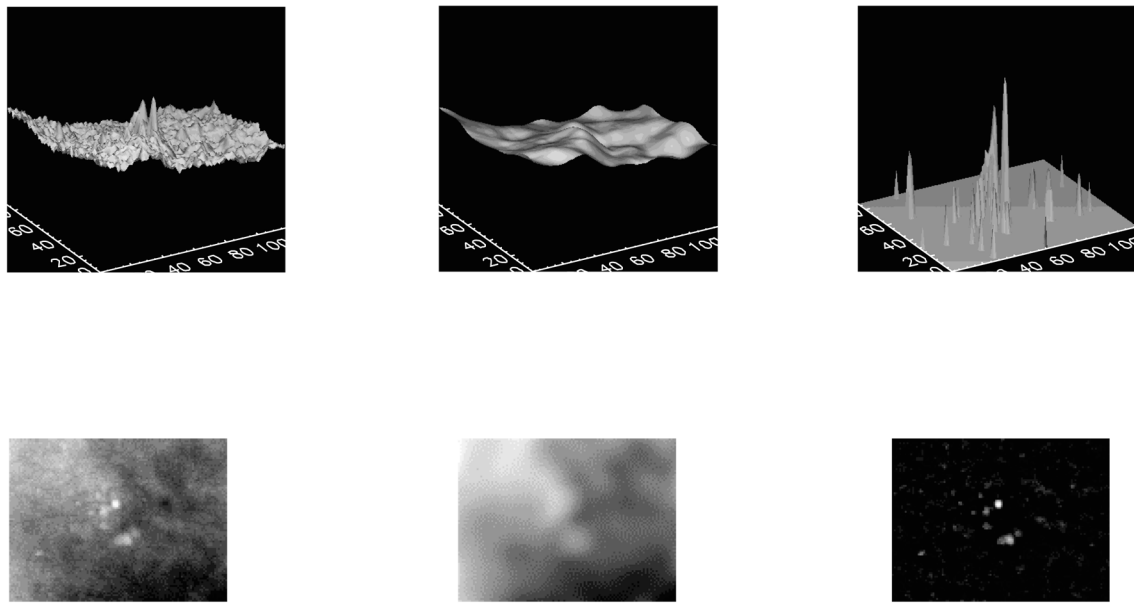

Fig. 1. Regional background correction: in the upper row a 3D representation of grey values within a kernel of size 27 by 27 is shown, while the lower one shows the corresponding image area. In the left column the original area is depicted, in the middle one the fitted polynomial, while the left one shows the image result after subtraction of the fitted polynomial from the original area. After subtraction the background is suppressed.

MCS. All patients had surgical biopsies to confirm if breast cancer was present. Histologic examination of the specimen revealed malignancy in 54 patients.

All 272 films were digitized with the Pixelizer 6k (Medical Diagnostic Computing, Zeiss, Hannover, Germany). A pixelsize of 91.5 μm was used for image processing. The bit depth was 15 bits (32768 shades of grey).

The mammographic appearance of the biopsied MCS were rated retrospectively on a 3 point scale: benign (n=13), indeterminate (n=5) and malignant (n=29) by two experienced radiologists (E.S., F.S.).

Suspicious areas which might contain a tumor were manually marked in all film projections of all 100 patients. Coordinates of the enclosing rectangle were saved. Groundtruth was established by labeling of 828 individual MCS, 97 film-folly-errors and 638 false positive appearing bright spots (e.g. crossing of septal lines or calcified vessels). Only one projection per patient was used in order to avoid redundancy. Furthermore, in 64 patients all clustered MCS, whether within the tumor area or not, were marked manually (n=134) in one projection.

Image processing consisted of the 3 following steps: 1) background correction, 2) detection and 3) classification. Each will be described within its own section. A total number of 4 different artificial neuronal nets (ANN) type backpropagation were used. One was applied within step 2 (detection of individual MCS) and three others within step 3 (one for identification of indeterminate clusters, one for classification of the remaining clusters, benign or malignant and another one for classification of all patients' clusters benign or malignant).

Step 1: Section background correction:

Background correction was achieved by fitting a two dimensional 3rd degree polynomial function within an area of 27 by 27 pixels around every pixel. The fitted area was then subtracted to suppress the background structure (Fig. 1).

Step 2: Detection:

The original image was high pass filtered using a kernel size of 9 by 9. Both, the high pass filtered image and the background corrected image were thresholded with the 98.5 percentile and saved as bi-level images. After multiplication of both bi-level images, the zeroes represented the background, and the ones pixels of potential microcalcifications. Sets of non- zero pixels within a four-neighbour region were labelled with a unique region index using an algorithm called "blob colouring" [13]. These regions represented potential microcalcifications. For all pixels of these regions the gradients in the x and y direction were calcu-

Fig. 2. Rotating individual MCS: upper and lower rows show MCS before and after rotation, respectively. MCS were rotated in such a way that their main axes become parallel to the horizontal direction.

lated, using the Sobel operators within a kernel size of 3 by 3 [14]. The computed gradients were transformed to angles and mapped to one of the 16 main directions [8]. Then a histogram of the mapped directions was obtained within a kernel of size 9 by 9. If this histogram showed two peaks in approximately opposite directions (i.e. if the difference between the two peaks was more than 6/16 and less than 10/16) then the values forming these peaks were multiplied with each other and stored as the line feature value of this particular pixel. Whenever 2 peaks were not identifiable, the line feature value was set to zero. Edge gradients of the regions were represented by the absolute value of the Sobel operators at the border pixels of objects.

Region contrast was defined as the difference between the average gray level value of the region and that of two pixel layers around the same object.

Descriptive statistics (minimum, maximum, average and variance) of the gray values, line fea-

tures, and edge gradient values of individual pixels forming a region were computed. These 12 features and the region contrast served as input to a three layer ANN (one hidden layer).

The ANN was trained by the established ground-truth data to differentiate between MCS and artifacts.

Step 3: Section Classification:

It was decided to characterize whole clusters as benign, indeterminate or malignant by training two different ANN's. For this purpose 73 properties were derived from the automated detected, clustered microcalcifications. Only microcalcifications located within the tumor area were used for feature calculation.

In detail, the automatically detected microcalcifications were rotated by the Hotelling transformation so that their main axes became horizontal to make their shapes and extension comparable (Fig. 2) [15]. This procedure was followed by the computation of the shape parameters,
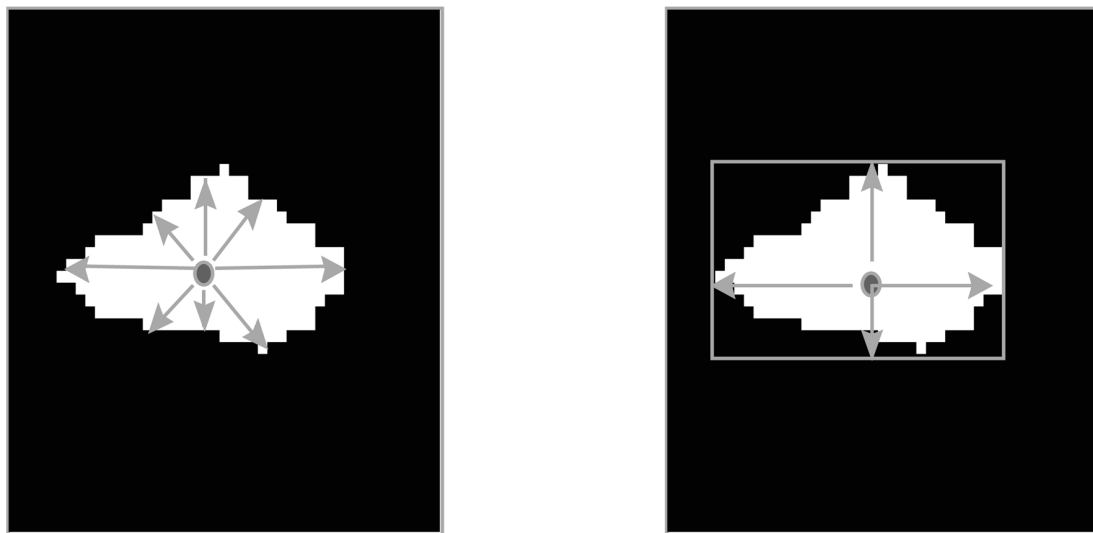
Fig. 3. Left image part exhibits the shape indices and their extension in 8 directions (arrows). The center of mass pixel is represented by the grey circle. The right image part demonstrates parameters derived from the minimum enclosing rectangle of an individual microcalcification: eccentricity is characterized by the distance to the borders of minimum enclosing rectangle (arrows).

consisting of the area (a), perimeter (p), and circularity (p^2/a) of the individual microcalcification. The shape indices were determined by the extension of a microcalcification along 8 main directions (Fig. 3). The ratio between the variance of all shape indexes of a microcalcification and their average value were computed as well. Further, the length (l), width (w), aspect ratio (l/w), and area (l*w) of the minimum enclosing rectangle and the eccentricity were computed (Fig. 3). In addition, for each individual microcalcification the descriptive statistics (minimum, maximum, average, standard deviation and variance) of gray levels, the response to high pass filtering, the border gradients as well as the region contrast were added to the feature set.

Finally the automated detected microcalcifications were grouped to form clusters, following the rule that within an individual cluster the distances between microcalcification are less than one centimeter. This procedure enabled us to derive the following properties.

For every microcalcification the minimum distance to the next nearest microcalcification, as well as the 25th, 50th and 75th percentile of distances to all MCS of the same cluster, were determined.

For every cluster descriptive statistics (minimum, maximum, average, standard deviation and range) were computed from the follow-

ing individual microcalcification features: area, perimeter, circularity, and distances between microcalcification as well as the extension in the horizontal direction.

FEATURES FOR IDENTIFICATION OF INDETERMINATE CLUSTERS (n=10)
number of MCS within cluster
maximum of MCS areas within the same cluster
range of MCS areas within the same cluster
maximum of MCS perimeters within the same cluster
range of MCS perimeters within the same cluster
maximum of MCS circularities within the same cluster
range of MCS circularities within the same cluster
variance of inter MCS distances within the same cluster
cluster area
cluster perimeter

Table 1.

FEATURES FOR IDENTIFICATION OF INDETERMINATE CLUSTERS (n=10)
number of MCS within cluster
maximum of MCS areas within the same cluster
range of MCS areas within the same cluster
maximum of MCS perimeters within the same cluster
range of MCS perimeters within the same cluster
maximum of MCS circularities within the same cluster
range of MCS circularities within the same cluster
variance of inter MCS distances within the same cluster
cluster area
cluster perimeter

Table 2.

The extension of a cluster was calculated according to the convex hull procedure (Fig. 4) [16]. The area (a), the perimeter (p), the circularity (p^2/a) of a cluster, the number of microcalcifications (n), and the density of microcalcifications within a cluster (n/a) were calculated.

The predictive power of individual features was measured by using the leave-one-out test and receiver operator characteristics (ROC) analysis [17]. For every individual feature a separate ANN was trained and afterwards a patient-based leave-one-out test was performed. There were two targets for ANN training: a) to identify indeterminate clusters according to the radiological rating and b) to classify the remaining clusters into the benign or malignant according to the histological report. The test results were saved and afterwards a ROC curve was created for every feature. Only those features, whose ROC curve crossed the first median at any time were chosen, i.e. those which predicted the patient target better than they predicated his/her chance. The final feature set (n=10) used as input of the ANN for identification of indeterminate clusters is listed in Table 1. Features used as input of the ANN for classification (n=12) of clusters into benign or malignant are depicted in Table 2. All ANN used within the classification step consisted of three layers (one hidden layer).

Performance of the used ANN's was estimated using a patient-based leave-one-out test. Quantification of results followed ROC analysis and the area under the ROC curve (Az value) was computed using a PC version of a software program (labroc1.exe) freely distributed by the Rossmann Institute, Univ. of Chicago, USA (ftp: random.bsd.uchicago.edu) [17]. Since a tumor area may contain more than one cluster of MCS, the performance was measured on per cluster basis. Therefore, for each patient the network outputs from cluster classification were averaged and a new ROC curve was constructed. Only the patient-based results will be shown. Every point of the ROC curve depicts a couple of sensitivity and specificity. Therefore,
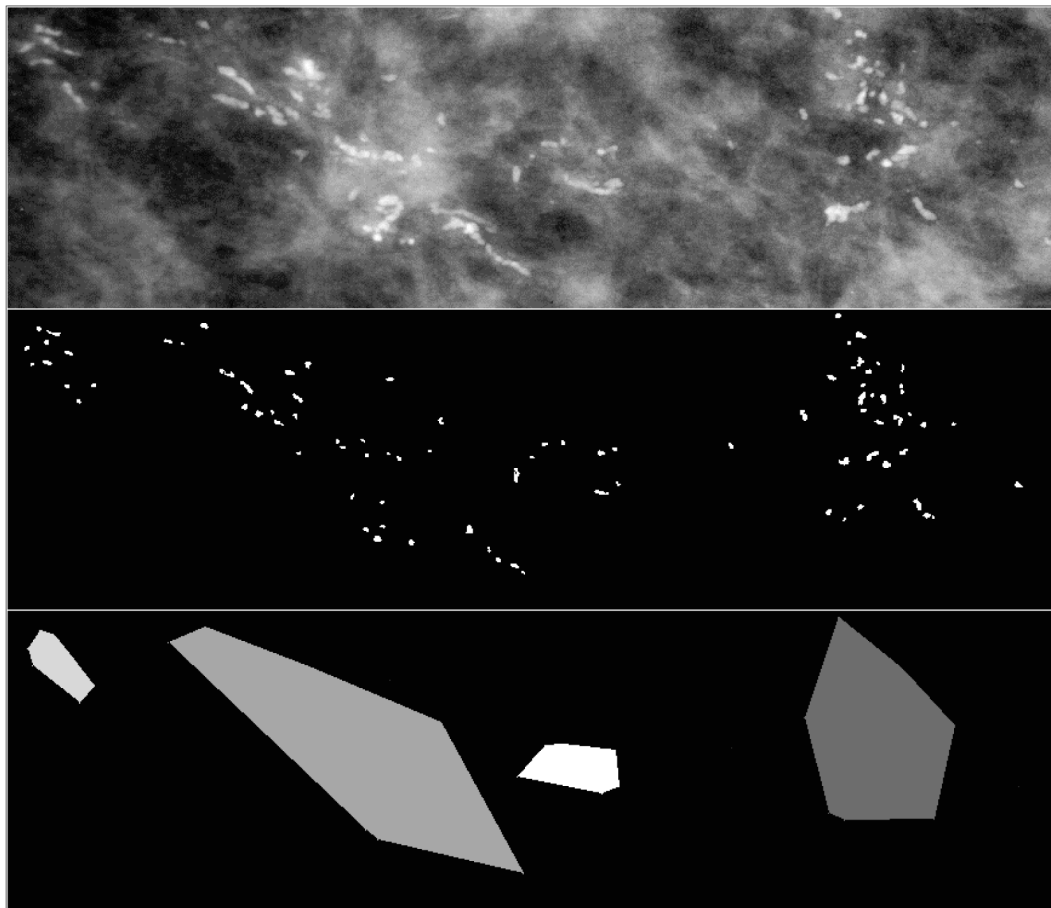
Fig. 4. The upper row of the figure shows the original image of a tumor area containing clustered MCS, the middle row depicts the MCS found automatically by the CAD system and the lower row shows the convex hull of clusters identified by the system.

for computation of sensitivity, specificity, negative and positive predictive powers, a particular point of ROC was chosen, which represented the best trade off between reasonable sensitivity and acceptable specificity.

The utilized hardware included a SunSparc 20 workstation (Sun Microsystems, Mount View, California) and the recently developed neurocomputer Synapse-1 (Siemens Nixdorf Advanced Technologies, Dresden, Germany), connected to the Sun workstation using the SBus adaptor. Synapse-1 was programmed through a special C++ library (Neural Algorithms Programming Library 1.3.3, Siemens Nixdorf Advanced Technologies, Dresden, Germany). Image processing was done with the help of IDL 4.0 (Interactive Data Language, Creaso Research Systems, Inc., Boulder, Colorado, USA).
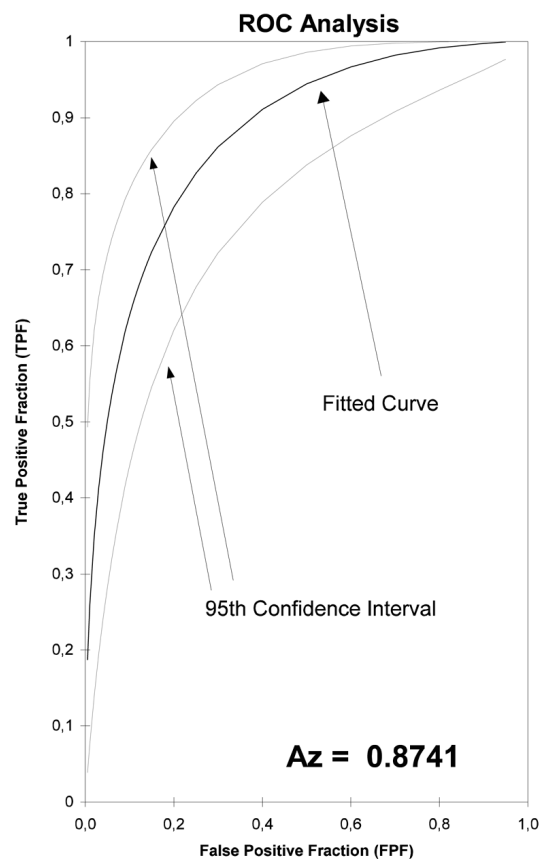

Fig. 5. ROC curve obtained on a per patient basis for identification of indeterminate clustered MCS.

ROC Analysis

True Positive Fraction (TPF)

Fitted Curve

95th Confidence Interval

Az = 0.8749

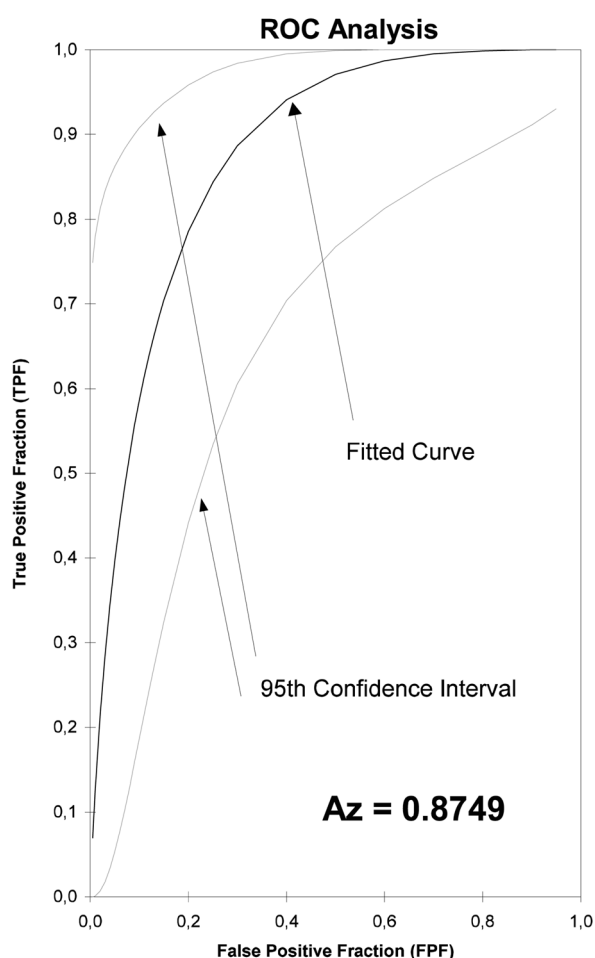**False Positive Fraction (FPF)**

Fig. 6. ROC curve obtained on a per patient basis for classification of malignant vs benign clustered MCS after identification of indeterminate clusters.

Results

For detection of MCS sensitivity values of 0.90, 0.98 and 1.00 at the respective false positive alarm rates of 1.3, 5.3 and 7.4 groups per image were achieved.

For identification of indeterminate clusters an Az-value of 0.8741 with a sensitivity of 0.977, specificity of 0.34 and accuracy of 0.7095 (ROC curve at Fig. 5) could be obtained on a per patient basis. A positive predictive value of 0.6715 and a negative predictive value of 0.9146 was calculated.

Classification of the remaining clusters into benign or malignant yielded the following results. For each patient a based classification of an Az-value of 0.8749 with a sensitivity of 0.977, specificity of 0.471 and accuracy of 0.8083 (see the ROC curve in Fig. 6) was achieved. Positive and negative predictive values were found

to be 0.787 and 0.911 respectfully. Using clusters of all patients for classification into benign or malignant ones an Az value of 0.64 could be obtained.

Discussion

The use of artificial neural nets for pattern recognition is well documented in radiology [18,19,20,21,22]. Artificial neural nets have been used to assist in differentiation of neonatal chest diseases and estimation of bone age in pediatrics [23,24]. Additionally, the usage of ANNs is reported in pulmonary nodule detection [25,26] and in scintigraphy [21,27].

So far studies dealing with computer-assisted mammography have focused mainly on the detection of clustered MCS [2,7,8,9]. The objective of this study was not only to investigate automated detection of clustered MCS, but also the computer-assisted classification of images containing clustered MCS with ANNs. Both, detection and classification of MCS have been performed automatically. Since it is known that "double reading" can improve the accuracy of medical reports by 5-15%, it is envisioned that a system of computer-aided diagnosis (CAD) could be used not to replace the radiologist, but rather to serve as a cost effective, never tired "virtual second reader" [6,28,29,30].

The achieved performance results in the detection task are comparable to those of other reports [2,7]. However, the recommended algorithm for performance measurements labels a cluster as true positive if at least two automated detected MCS are found within the previously marked area. But this does not necessarily mean that an individual MCS was really situated on that particular position. If two false positive detected MCS were located within the marked area, the cluster was regarded as true positive [7].

Another approach to assess the performance of a detection scheme is to find out whether the detected MCS can serve as the input of a computer system whose aim is to classify clustered MCS as benign or malignant. In contrast to other studies mentioned in this paper this was exactly our approach, i.e. we used only automatically detected MCS in the classification step. Similar to the radiologic film interpretation, for a given

patient all clusters of MCS were classified by our CAD system.

Reliable results of automated classification could be achieved for the retrospectively rated benign or malign clustered MCS. Since all patients of the database were operated due to the attending radiologist's suspicion of malignancy, the high negative predictive value of 0.911 implicates that there is a chance for the CAD system to spare women with histologically benign diseases from biopsy. Psychological and physical stress as well as medical costs might be reduced.

When training an ANN with all clusters of all patients for the differentiation between benign and malignant cases, an Az of 0.64 was achieved. This reflects that the generalization ability of the CAD system is still poor. The reason might be that features derived from binary transformation of medical expert knowledge by digital image processing cannot give better results than the human observer itself. This is supported by a report, where nine radiologists reached an Az value of 0.77 for rating clustered MCS in 77 mammographic films [31].

A possible solution would be to use a two step procedure. The first step would be to identify indeterminate clusters, which should undergo further human brainstorming or additional investigations like magnifying views, ultrasound studies, magnetic resonance imaging or interventional procedures. An Az value of 0.8471 obtained for identification of indeterminate clusters shows that our CAD system seemed to be able to identify those cases.

The authors are aware of the fact that the prototype developed is just one element of the "virtual second reader" since at the moment the developed CAD system handles only the clusters containing MCS. Soft tissue masses without MCS cannot be detected and classified. This has to be implemented in the furture.

In conclusion, a fully automated CAD system was developed. Clustered MCS, identified by a detection scheme, are used as a source of the data for computer-assisted classification. The CAD system is able to identify indeterminate cases and produces a reliable estimation of biologic dignity for the remaining ones. Future work will be directed towards validating the reliability of these results in daily clinical routine.

A prospective trial is currently being started at our institution. The CAD system is further being adapted to various environment variables like different ie. film-folly types, different scanning devices and/or digital mammographic imaging.

References

[1] R. A. SCHMIDT, *The Epidemiology of Breast Cancer*, In Kopans DB. Mendelson EB, Syllabus: A Categorial Course in Breast Imaging, RSNA 1995, 7–20.

[2] Y. WU ET AL., Computerized detection of clustered microcalcifications in digital mammogramms: Applications of artificial neural networks, *Medical Physics* **19** (3) (1992), 550–560.

[3] E. S. DE PAREDES ET AL., Mammographic and histologic correlations of microcalcifications, *Radiographics*, **10** (4) (1990), 577–589.

[4] J. P. HOGGE ET AL., The mammographic spectrum of fat necrosis of the breast, *Radiographics*, **15** (6) (1995), 1347–1356.

[5] B. S. MONSEES, Evaluation of breast microcalcifications, *Radiologic Clinics of North America*, **33** (6) (1995), 1209–1221.

[6] R. A. SCHMIDT ET AL., *Computeraided Diagnosis in Mammography*, In Kopans DB. Mendelson EB, Syllabus: A Categorial Course in Breast Imaging, RSNA 1995, 199–207.

[7] N. KARSSEMEIJER, Adaptive noise equalization and recognition of microcalcification clusters in mammograms, *International Journal of Pattern Recognition and Artificial Intelligende*, **7** (1993) 1357–1376.

[8] N. KARSSEMEIJER, A stochastic model for automated detection of calcification in digital mammograms, *International Journal of Information Processing in Medical Imaging 1*, (1991), 227–238.

[9] W. P. KEGELMAYER, M. C. ALLMEN, *Dense Feature Maps for Detection of Calcifications*, In Gale AG, Astley SM, Dance DR, Cairns AY, Digital Mammography, Excerpta Medica 1994, 3–12.

[10] J. A. BAKER ET AL., Breast cancer: prediction with artificial neural network based on BI-RADS standardized lexicon, *Radiology* **196** (1995), 817–822.

[11] Y. A. JIANG ET AL., Malignant and Benign Clustered Microcalcifications: Automated Feature Analysis and Classification, *Radiology*, **198** (1996), 671–678.

[12] Y. WU ET AL., Artificial neural networks in mammography. Application to decision making in the diagnosis of breast cancer, *Radiology*, **187** (1) (1993), 81–87.

[13] C. F. GONZALEZ, R. E. WOODS, "Representation and Descirption" in *Digital Imaging Processing* edited by C. F. Gonzalez, R. E. Woods (Addison-Wesley-Publishing Company, (1993), 418–420.

[14] C. F. GONZALEZ, R. E. WOODS, *Digital Imaging Processing* 3rd ed., Addison-Wesley-Publishing Company, (1992), 418–420.

[15] C. F. GONZALEZ, R. E. WOODS, *Digital Imaging Processing* 3rd ed., Addison-Wesley-Publishing Company, (1992), 148–156.

[16] C. F. GONZALEZ, R. E. WOODS, *Digital Imaging Processing* 3rd ed., Addison-Wesley-Publishing Company, (1992), 490–491.

[17] C. METZ, Some Practical Issues of Experimental Design and Data Analysis in Radiological ROC studies, *Investigative Radiology*, **24** (1989), 234–245.

[18] J. M. BOONE, Neural networks at the crossroads, *Radiology*, **189** (1993), 357–359.

[19] J. M. BOONE, Sidetracked at the crossroads, *Radiology*, **193** (1994), 28–30.

[20] C. E. KAHN JR., Artificial intelligence in radiology: decision support systems, *Radiographics*, **14** (1994), 849–855.

[21] J. A. SCOTT, E. L. PALMER, Neural Network analysis of ventilation–perfusion scans, *Radiology*, **186** (1993), 661–675.

[22] R. SCHIER, Neural Networks, *Radiology*, **191** (1994), 291.

[23] G. W. GROSS ET AL., Neural Networks in radiologic diagnosis: II. Interpretation of neonatal chest radiographs, *Investigative Radiology*, **25** (1990), 1017–1023.

[24] G. W. GROSS ET AL., Pediatric Skeletal Age: Determination with neural networks, *Radiology*, **195** (1995) 689–695.

[25] J. W. GURNEY, S. J. SWENSEN, Solitary pulmonary nodules: determining the likelihood of malignancy with neural network analysis, *Radiology*, **196** (1995) 823 ff.

[26] Y. C. WU, Detection of lung nodules in digital chest radiographs using artificial neural nets: pilot study, *Journal of Digital Imaging*, **8** (1995), 88–95.

[27] R. E. FISHER, E. L. PALMER, Neuronal networks in ventilation - perfusion imaging: part I. Effects of interpretive criteria and network architecture, *Radiology*, **198** (1996), 699–706.

[28] R. E. BIRD, Professional quality assurance for mammography screening programs, *Radiology*, **177** (1990), 8–10.

[29] E. L. THURFJELL ET AL., Benefit of independent double reading in a population-based mammography screening program, *Radiology*, **191** (1994), 241–244.

[30] L. TABAR ET AL., Update of the Swedish two-county programof mammographic screening for breast cancer, *Radiological Clinics of North America*, **30** (1992), 187–210.

[31] W. VELDKAMP, N. KARSSEMEIJER, *Automated Classification of Clustered Microcalcifications in Digital Mammography*, In Doi K, Digital Mammography, Excerpta Medica (1996), 23–30.

Contact address:
Erich Sorantin
Department of Radiology
Univ.Hospital Graz
Auenbruggerplatz 34
A - 8036 Graz
Austria
phone: 0043 / (0) 316 / 385 - 4225
Fax: 0043 / (0) 316 / 385 - 4299
e-mail: `erich.sorantin@kfunigraz.ac.at`

ERICH SORANTIN was born in 1957. After finishing the high school in 1976 he studied medicine at the University of Vienna. Promovation was in March 1982. In the later course he was trained as general practioner and in the medical subspeciality of Pediatrics. In 1988 he joined the Department of Radiology, Univ. Hospital Graz for further specialisation in Radiology with a focus on Pediatric Radiology. In 1994 he become the Vicehead of the Section of Pediatric Radiology and in 1995 the head of the Division for Digital Information and Image Processing. During 1995 to 1996 he took part in the European Research Project SYNAP9301, dealing with Neurocomputing. He holds the position as a consultant regarding computer graphics in medicine for 3 companies. His scientific interest were always targeted in biosimulation, expert systems and image processing. Papers and congress contributions were dealing with expert systems for mechanical ventilation in newborns, automated detection of breast cancer in digitised mammographie s (breast xray images) and the application of Virtual Reality in Radiology including virtual endoscopy.

FERDINAND SCHMIDT was born in Graz, Austria in 1961. After he finished High School in Graz in 1980 he started to study medicine at the Karl-Franzens University in Graz. Between 1985 and 1987 he stayed in Japan mainly at the Department of Radiology in the University Hospital in Niigata. This scholarship was sponsored by the Japanese Ministry of Education, Monbusho. He received his Dr. med. univ. degree in 1998. In 1990 he became a resident at the University Hospital Graz, Department of Radiology where he was board certified in 1995. During his residency his main scientific interest was the field of mammography in various aspects like screening, MR imaging of the breast, interventional methods and especially the field of Digital Mammography and CAD. In 1999 he received his Ph.D.

HEINZ MAYER was born in Graz, Austria in 1968. After he graduated from the Technical High School for Telecommunication Engineering and Electronics in Graz he studied Telematics at the University of Technology, Graz in 1987. He received his Dipl.-Ing.-degree in Telematics (special topic Computer Graphics) from the same university in 1996. From October 1995 to June 1996 he served his military service in the Austrian Army.

After 1 year at the Radiology Department of the University Hospital Graz, where he worked in the field of Digital Mammography and Virtual Endoscopy, he joined the Computer Graphics and Vision Department of the University of Technology in Graz. His research interests include computer graphics related measurements on materials (BRDF, texture), medical volume visualization and augmented reality applications.

MICHAEL BECKER studied Technical Mathematics and graduated 1986 in Graz. In 1995 he participated in an EC-project dealing with automated detection and classification of microcalcifications in mammograms by means of neuronal networks. Since then he is employed in the IT-Department of the Styrian hospitals as coordinator for implementing hospital-related software-applications.

CSABA SZEPESVÁRI received his Ph.D. degree in mathematics from JATE, Szeged, in 1999. He is the holder of the Pro Sciencia Golden Legature in Computer Science. After finishing his Ph.D. studies at the Bolyai Institute of Mathematics, JATE, Szeged, he worked as a researcher and lecturer in the Research Group on Artificial Intelligence of the same university where he developed algorithms to control autonomous robots, which were tried out on a real-robot. He was the invited speaker at several conferences, organized conference sessions and is a member of the international program committee of several conferences. He has published more than 20 articles in refereed international journals, one book chapter and several patents.

He joined Mindmaker Ltd. (previously known as Associative Computing, Ltd.) in October 1997.

PETER WINKLER was born in Bruck, Austria in 1969. He finished high school in Klagenfurt in 1988 and graduated in Technical Physics at the Technical University Graz in 1997. From 1997 to 1998 he worked at the Division of Digital Information and Image Processing, University Hospital Graz, in the fields of Digital Mammography and Virtual Endoscopy. Since 1998 he is employed as a Medical Physicist at the Divsion of Radiotherapy at the same hospital. His current research project is Digital Images processing quality assurance for stereotactic Radiosurgery.